Design and characterization of a new pressurized flat panel photobioreactor for microalgae cultivation and CO2 bio-fixation

Design and characterization of a new pressurized flat panel photobioreactor for microalgae cultivation and CO_2 bio-fixation.

Michele Carone*[1], Davis Alpe[2], Valentina Costantino[1], Clara Derossi[1], Andrea Occhipinti[3], Mariachiara Zanetti[1], Vincenzo A. Riggio[1]

1: Department of Environment, Land and Infrastructure Engineering, Politecnico di Torino, Corso Duca degli Abruzzi 24, 10129 Torino, Italy

2: Photo B-Otic S.r.l., Via Paolo Veronese 202, 10148 Torino, Italy

3: Abel Nutraceuticals S.r.l., Via Paolo Veronese 202, 10148 Torino, Italy

* Correspondence to Michele Carone at michele.carone@polito.it

Abstract

Microalgae-based biorefinery processes are gaining particular importance as a biotechnological tool for direct carbon dioxide fixation and production of high-quality biomass and energy feedstock for different industrial markets. However, despite the many technological advances in photobioreactor designs and operations, microalgae cultivation is still limited due to the low yields achieved in open systems and to the high investment and operation costs of closed photobioreactors. In this work, a new alveolar flat panel photobioreactor was designed and characterized with the aim of achieving high microalgae productivities and CO_2 bio-fixation rates. Moreover, the energy efficiency of the employed pump-assisted hydraulic circuit was evaluated. The 1.3 cm thick alveolar flat-panels enhance the light utilization, whereas the hydraulic design of the photobioreactor aims to improve the global CO_2 gas-liquid mass transfer coefficient ($k_La CO_2$). The mixing time, liquid flow velocity, and $k_La CO_2$ as well as the uniformity matrix of the artificial lighting source were experimentally calculated. The performance of the system was tested by cultivating the green microalga *Acutodesmus obliquus*. A volumetric biomass concentration equal to 1.9 g L^{-1} was achieved after 7 days under

controlled indoor cultivation conditions with a CO_2 bio-fixation efficiency of 64 % of total injected CO_2. The (gross) energy consumption related to substrate handling was estimated to be between 27 and 46 Wh m^{-3}, without any cost associated to CO_2 injection and O_2 degassing. The data suggest that this pilot-scale cultivation system may constitute a relevant technology in the development of microalgae-based industrial scenario for CO_2 mitigation and biomass production.

Keywords

Flat panel photobioreactor, CO_2 mass transfer coefficient, CO_2 bio-fixation efficiency, Hydrodynamic characterization, *Acutodesmus obliquus*.

1. Introduction

Since the 20th century, the concentration of greenhouse gases in the atmosphere continued to increase as result of anthropogenic activities related to the use of fossil fuels, deforestation, and agricultural activities. The annual global average carbon dioxide concentration at Earth's surface in 2020 has reached 412.5 ± 0.1 ppm, the highest value in modern atmospheric records, increasing by 2.5 ± 0.1 ppm from 2019, a value comparable to the average rate of increase during the last decade (Blunden and Boyer, 2021). Therefore, the development of renewable and clean technologies is needed to sustain a considerable fraction of the global economy and to reduce the impact of human activities. In parallel, major efforts are needed to improve CO_2 Capture and Utilization (CCU) technologies that can effectively reduce carbon dioxide emissions mainly from power plants and different industrial processes.

In this context, microalgae-based refinery concepts have gained importance over the last few decades. Microalgae are considered promising biochemical factories and excellent CO_2 fixers (Brown and Zeiler, 1993). Their simple cellular structure, large

surface-to-volume ratio, and aquatic lifestyle allow these organisms an easy access to water, CO_2 and other nutrients, and thus a more efficient conversion of solar energy into chemical energy, showing 10-50 higher CO_2 fixation rates than land plants (Carlsson et al., 2007; Goli et al., 2016; Rosenberg et al., 2011). Moreover, compared to higher plants, microalgae also show faster growth rates and their cultivation does not compete for arable lands (Greenwell et al., 2010; Khan et al., 2009). As a result of CO_2 fixation, microalgae accumulate significant amounts of carbohydrates, proteins, lipids, and other valuable compounds, such as pigments and vitamins. Hence, microalgal biomass is considered a promising energy feedstock with multifaceted applications in the production of dietary supplements, cosmetics, food and animal feed and biofuels (Cheah et al., 2015; Francisco et al., 2010; Gimpel et al., 2015; Vanthoor-Koopmans et al., 2013). Algal cultivation technologies are traditionally classified as open or closed systems (photobioreactors, PBRs). Open cultivation systems (*e.g.*, artificial ponds, raceways, thin layer) produce algal biomass at lower costs thanks to their lower investment and management costs in terms of Capital Expenditure (CapEx) and Operating Expense (OpEx) (Benemann, 2013). The open raceway pond is currently the most frequently used and cheapest cultivation system for commercial production of microalgae (Acién et al., 2017). Despite this, the open pond technology is limited by several disadvantages such as low biomass productivities, mainly related to poor mixing, low CO_2 mass transfer, high risk of biological and chemical contamination and high consumption of water. Moreover, its dependence on climatic conditions limits its application to tropical and subtropical regions (Chini Zittelli et al., 2013; Pandey et al., 2014; Tredici et al., 2010). On the other hand, closed photobioreactors allow precise control of the operating conditions and show higher biomass productivities. The confined space limits contaminations and assures higher biomass quality, but requires higher CapEx and OpEx (Adesanya et al., 2014; Norsker et al., 2011). Currently, tubular photobioreactors are the most common closed

system configurations for industrial-scale microalgae cultivation, mainly related to high-value applications (Acién et al., 2017; Chini Zittelli et al., 2013; Torzillo and Zittelli, 2015). However, all types of closed systems present major constraints in the process scale-up, mainly due to the difficulty in increasing the sizes of PBRs while keeping optimal culture and hydrodynamic parameters. The choice of the circulating device and design of the PBR influences important operating parameters such as mixing time, turbulence degree, O_2 build-up, and CO_2 supply, thus impacting on both the overall performance of the process (Torzillo et al., 2003) and the final cost. An extensive comparison of the strengths and limitations of the different cultivation systems, together with the importance of illumination and hydrodynamic parameters, has been thoroughly analysed in several reviews (Acién et al., 2017; Carvalho et al., 2006; De Vree et al., 2015; Torzillo and Zittelli, 2015; Tredici et al., 2010; Yadav and Sen, 2017). It is important to note that, although many PBRs and open system setups have been proposed at laboratory and industrial levels, there is no optimal design for all applications. Moreover, the overall negative energy balance of the processes still poses limitations in the scale-up of microalgal culture technologies, making them profitable only for applications with high added value goods such as dietary supplement and cosmetic raw materials (Acién et al., 2012; Slade and Bauen, 2013; Tredici et al., 2015). Recently, several studies have focused on the development of many simulation approaches coupling computational fluid dynamics, mass transport phenomena and microbial growth kinetics, to identify the best conditions to maximize microalgae productivity (del Rio-Chanona et al., 2019; Solimeno et al., 2017; Tan et al., 2020; Vasile et al., 2021; Weise et al., 2019). Likewise, several new design of open, closed, and hybrid PBRs setups based on different hydrodynamics, mass transfer mechanisms and illumination strategies have been proposed to improve the global cultivation efficiency and the scale-up feasibility (Chen et al., 2016; Chiaramonti et al., 2013; Cuaresma et al., 2009; Estrada-Graf et al., 2020; Li et al., 2014; López-Rosales et

al., 2019; Massart et al., 2014; Reyna-Velarde et al., 2010; Rodolfi et al., 2009; Sierra et al., 2008; Tan et al., 2020; Tredici et al., 2015; Yadav et al., 2015). Particularly, more attention was given to flat panel PBRs due to the high photosynthetic efficiencies that can be reached (Jorquera et al., 2010). However, currently employed flat panel PBRs still present some limitations mainly due to the low mixing efficiency, being the air bubbled mainly directly from the bottom of the panels, which brings to high energy costs and can lead to the occurrence of serious biofouling (Sierra et al., 2008; Tredici et al., 2015). Moreover, the use of compressed air for mixing constitutes a major part of the PBR energy consumption. Indeed, the power supply associated to air compression is function of the type of compressor, gas pressure, type of blower, and the aeration rate (Norsker et al., 2012). Centrifugal pumps, which are considerably more efficient than air compressors, have been mainly employed in tubular PBRs, although the concern for cell shear damage has led more frequently to the use of air-lift pumps. Nevertheless, as pointed out by Norsker and co-authors, the use of centrifugal pumps would be not recommended only for the cultivation of very shear sensitive algae (Norsker et al., 2011). To our knowledge, no literature reports are present concerning pilot-scale flat panel PBRs with a centrifugal pump. In this research, it is presented the design and characterization of a novel alveolar flat panel photobioreactor with a pump-assisted hydraulic circuit, that constrains microalgae to flow inside a positive-pressurized serpentine directly exposed to the artificial light source. The system has been realized to maximize the distribution of light through the microalgae culture as the width of the flat panels is equal to 1.3 cm. The main purpose of this work was to assess the hydrodynamic and cultivation performances of the proposed PBR. The results will help to improve the actual proposed technology and to evaluate its possible use in an industrial scenario, in which the application of energy-efficient technologies is nowadays a priority.

Therefore, the hydraulic, lighting and energetic behaviour of the new flat-panel PBR were investigated through the experimental characterization of the hydraulic flow, mixing time, CO_2 gas-liquid mass transfer coefficient, and irradiance matrix. The biological performances of this new prototype were tested by cultivating the green microalga *Acutodesmus obliquus*.

2. Materials and Methods

2.1 The flat panel photobioreactor

The photobioreactor used in this research was kindly provided by Arcobaleno Cooperativa Sociale (Turin, Italy), the patent holder of the PBR (EP2830413A1). A representative scheme of the PBR is reported in Figure 1A. Briefly, it is composed by two interconnected units: a photostage loop and a mixing tank. The photostage loop consists of two parallel alveolar flat panels illuminated by an interposed array of seven fluorescent lamps (58W, OSRAM, Germany). The alveolar flat panels are made of transparent polycarbonate with a light exposed surface area of 1.5 m^2 each and an internal path of 13 mm. Each panel is partitioned into 28 internal channels (alveoli) for a total length of the illuminated path of about 40 m and total volume of about 17 L. The mixing tank is made up with a darkened HDPE (High density polyethylene) material with a total volume of 50 L. Its truncated-cone shape has been designed to minimize biomass sedimentation (Fig. 1B). The tank is equipped on its top of a hydraulic inlet and a removable lock cap. A hydraulic circulator (ALPHA1 L - 45W, Grundfos, Denmark) is connected at the bottom of the mixing tank and upstream of the photostage loop. The hydraulic circulator drives the liquid flow into both flat panels, from the bottom to the top. Moreover, the hydraulic circulator allows to manually set up three different factory-defined liquid flow rates operating with constant performance curves. Gas inlet coming from a food grade CO_2 tank is located between the bottom of mixing

tank and the hydraulic circulator. This configuration maximizes gas dissolution in the liquid phase thanks to the turbulence generated by the circulation system. CO_2 flow rates are finely regulated by a thermal flow meter (Red-y smart controller GSC, Vögtlin Instruments GmbH Switzerland), whereas temperature/pH, conductivity, dissolved oxygen, and carbon dioxide are constantly monitored by a InPro 325Xi pH electrodes, Four-electrode conductivity sensor, InPro 6000 Optical O_2 sensor and a InPro 5000i CO_2 sensor (Mettler-Toledo®, USA), respectively. The probes are located at the output of the flat panels. The PBR is equipped with a Mettler-Toledo® multi-parameter transductor M800 and the signals from the sensors are transmitted to a Programmable Logical Controller (PLC, Unitronics, Israel) through industrial standard analogic signal protocol (4-20 mA). The PLC controls a dedicated solenoid valve for the CO_2 injection, allowing the regulation of the CO_2 flow based on pH or carbon dioxide concentration threshold, according to the experimental setup. A schematic overview of the whole PBR working process is reported in Figure 2.

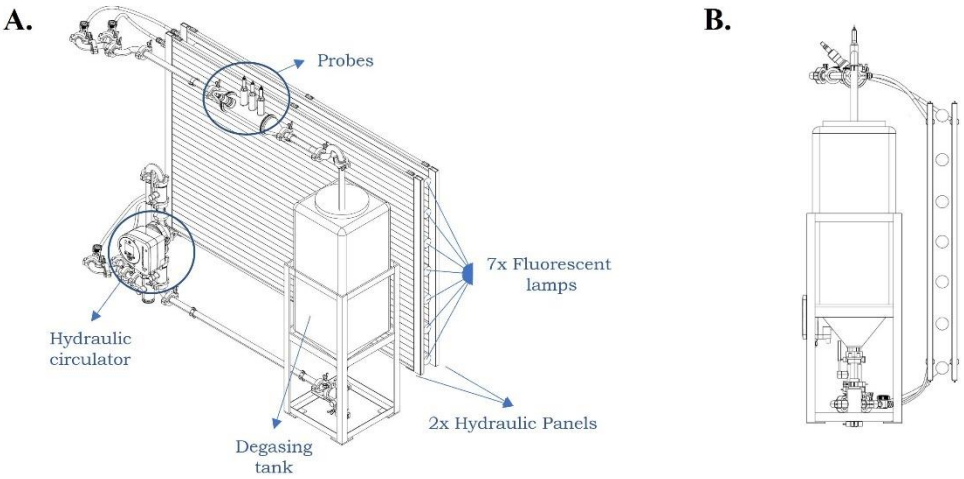

Figure 1: Schematic representation of the flat panel photobioreactor. A) 3D isometric view of the whole PBR. B) Schematic view of the mixing tank.

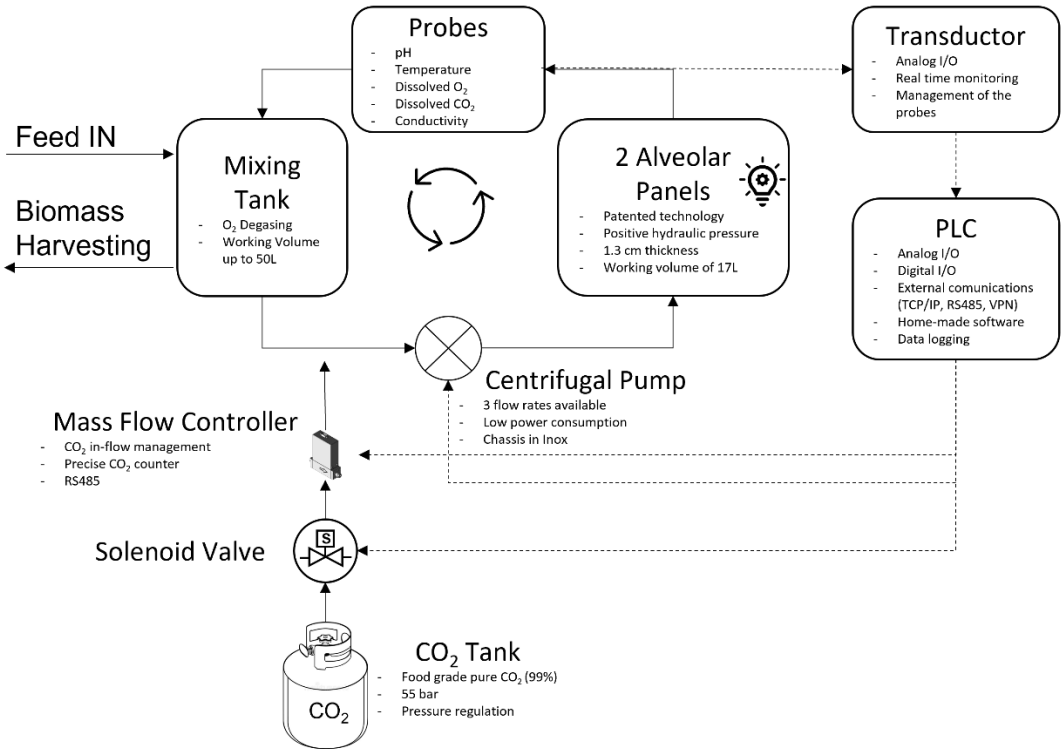

Figure 2: Schematic process diagram of the flat panel photobioreactor.

2.2 Microalgae and cultivation conditions

Acutodesmus obliquus strain 276-3b, formally *Scenedesmus obliquus* (Turpin) Kützing, was obtained from the SAG Culture Collection of Algae (Göttingen, Germany). The inoculum preparation was carried out in batch mode and axenic conditions in 2 L disposable culture chambers by using a 1.5 L volume of sterile BG-11 medium (Stanier et al., 1971). The cultures were maintained at constant temperature (23°C ± 2), pH 7.00-7.50, and under constant (24/24 h of illumination) artificial illumination (120 μmol m^{-2} s^{-1}) by fluorescence tubes (Osram, Germany). Aeration and mixing of the cells were guaranteed by flowing air at the bottom of the chambers. The microalgal cells were used to inoculate the flat panel photobioreactor when they just reached the stationary phase. The PBR was inoculated with BG-11 medium and microalgae cells for a total volume of 60 L, corresponding to a surface area-to-volume ratio (S_f/V) of 50 m^{-1}, and an initial cell concentration of 0.25 g L^{-1} of dry weight. Each experiment in the PBR was conducted in

batch mode for 7 days. The injection of CO_2 was carried out with a flow rate of 0.12 L min^{-1}, keeping constant the CO_2 concentration threshold in the PBR at 25 mg L^{-1} using the combination of solenoid valve and mass flow meter.

2.3 Biomass concentration measurements

Microalgae growth was gravimetrically quantified as dry biomass concentration as previously reported (Perin et al., 2017). Briefly, 10-20 mL of microalgae culture was filtered using pre-weighted 1.5 µm pore size glass fibre filters (Hahnemühle, Germany). The filters were then dried using a thermobalance (MLS-N, Kern, Germany) until stable weight, and then weighted with an analytical balance (Kern, Germany).

The biomass volumetric productivity (P_x) was then calculated as [Eq. 1]:

$$P_x = \frac{X_t - X_0}{t - t_0} \quad (1)$$

where X_t is the biomass concentration [g L^{-1}] at time t [d], and X_0 is the biomass concentration [g L^{-1}] at time t_0 [d].

2.4 Hydraulic flow determination

The hydraulic flow rate of the hydraulic circulator was measured using an electromagnetic flow meter (FD-Q20C. Keyence, Japan). All measurements were carried out by placing the flow meter at the outlet of the hydraulic panels.

2.5 CO_2 mass transfer coefficient ($k_La CO_2$)

In order to estimate gas-liquid transfer efficiencies of the photobioreactor, the $k_La CO_2$ was measured using 60L of distilled water (without microalgal cells) to avoid interferences of biological activity. The test was conducted at room temperature and atmospheric pressure (25 ± 2°C and 101.325 Pa).

The tests were conducted by blowing a constant and continuous flow rate of CO_2 inside the PBR and monitoring, through the CO_2 probe, the carbon dioxide concentration over time. Different carbon dioxide flow rates were tested at different hydraulic circulator powers (different hydraulic flow rate). As indicated in paragraph [2.1], the PBR employs a circulation system that allows to choose between three different levels of power flows corresponding to three different liquid rates. For each circulation level, the k_La value was identified for different carbon dioxide flow rates.

The $k_La CO_2$ parameter was determined using the following equation [Eq. 2](Sierra et al., 2008):

$$\frac{dC}{dt} = k_L a * (C^* - C) \quad (2)$$

integration for $C = C_0$ at $t = 0$ lead to [Eq. 3]:

$$\ln\left(\frac{C^* - C}{C^* - C_0}\right) = -k_L a * t \quad (3)$$

where C_0 is the initial CO_2 concentration [mg L^{-1}], C is the dissolved CO_2 concentration [mg L^{-1}] at time t, C^* is the CO_2 saturation concentration in water [mg L^{-1}] and t is time [min]. Since dissolved carbon dioxide is in equilibrium with carbonate and bicarbonate species, to determine the exact concentration of carbon dissolved into the aqueous phase the relevant equilibrium and corresponding equilibrium constants were calculated as previously reported (Chen et al., 2016).

2.6 CO_2 fixation yield

The CO_2 fixation yield (ηCO_2) expresses the CO_2 bio-fixation rate of the culture in terms of percentage (Lim et al., 2021). It is calculated as the ratio between the kilograms of carbon accumulated within the algal biomass at the end of the cultivation and the kg of

carbon supplied to the microalgae through the injection of CO_2 at a known flow rate [Eq. 4], as previously reported (Lim et al., 2021).

$$\eta CO_2 = \frac{W_{C\ biomass}}{W_{C\ in}} * 100 \quad (4)$$

With $W_{C\ biomass}$ and $W_{C\ in}$ deriving respectively from [Eq. 5] and [Eq. 6]:

$$W_{C\ biomass} = W_{biomass} * C_{C\ biomass} \quad (5)$$

$$W_{C\ in} = (W_{CO2\ in} - W_{CO2\ water}) * (M_C/M_{CO2}) \quad (6)$$

Where $W_{C\ biomass}$ is the kg of carbon accumulated in the biomass; $W_{biomass}$ the kg of biomass obtained during the cultivation; $C_{C\ biomass}$ is the fraction of carbon within the cells obtained through experimental elemental analysis of *A. obliquus*; $W_{C\ in}$ is the kg of carbon injected into the PBR as CO_2 flow; $W_{CO2\ in}$ is the total kg of CO_2 injected; $W_{CO2\ water}$ is the kg of CO_2 dissolved in water at the end of the batch; M_C and M_{CO2} represent respectively the molar mass of carbon (12 g mol^{-1}) and carbon dioxide (44 g mol^{-1}).

2.7 Mixing time

The mixing time [t_m] is defined as the time required to attain a given uniformity close to the fully mixed state after the injection of a tracer (Yang and Mao, 2014) and it was evaluated by a pH tracing test. To estimate the mixing time of the photobioreactor, the experiments were performed using 60 L of distilled water (without microalgal cells) to avoid interferences of biological activity. Diluted hydrochloric acid (5 mL HCl; with a final concentration in the PBR of 10^{-3} M) was poured into the mixing tank of the photobioreactor, and the pH was recorded every minute by the pH probe located at the

output of the flat panels. The t_m was determined as the time required to reach the 95% of complete homogeneity after the injection of the HCl solution (Chisti, 1989).

2.8 Energetic measurements

The energy consumption of the PBR main components (hydraulic circulator and lighting system) was measured using a digital multimeter (Siglent SDM3065X-SC, Germany). Voltage and current intensity measured for each unit were used to calculate the power input expressed in Watt [W]. These data, together with the hydraulic flow measurements, were further computed to evaluate the net energy consumption for the fluid handling as Wh m^{-3}.

2.9 Radiance matrix

The PBR was illuminated by an artificial lighting system based on an array of seven fluorescent tubes interposed between the two flat panels. To evaluate the uniformity of incident light on both exposed surfaces of the panels, the light intensity was determined by a PAR spectroradiometer (PLA 20, Everfine, China). A matrix array was imposed on the artificial lighting system to fix and homogeneously distribute the sampling points along the radiant surface. The data obtained from the measurements were interpolated using the software Matlab® to create the pattern of light intensity for the whole exposed panel surface.

The light uniformity coefficient was calculated using the following equation:

$$U_I = \frac{I_{min}}{I_{mean}} \times 100 \quad (7)$$

where U_I is the light uniformity coefficient [%], I_{min} is the minimum value of light intensity [µmol m^{-2} s^{-1}] and I_{mean} is the mean value of light intensity [µmol m^{-2} s^{-1}].

3. Results and discussion

3.1 Hydrodynamics flow description

This study has described, for the first time in literature, the hydrodynamics, mass transfer and mixing time parameters of an innovative and patented flat panel photobioreactor. The experimental characterization of biological performance parameters has been also reported. Key hydrodynamic parameters have been explored in order to compare the pump-assisted setup of the cultivation system here reported to traditional flat panel photobioreactors. In the latter, mixing and liquid flow is typically achieved by air bubbling or through an external airlift system. Whereas the hydrodynamics of the described PBR is function of the pump-driven culture flow, and thus is linked to the gross power of the hydraulic circulator. Therefore, the hydrodynamics characterization of the reactor included the measurements, at the three default pump setups and at various CO_2 injection rates, of the different liquid flow rates and the effects on the mixing time and the CO_2 volumetric mass transfer coefficient ($k_La CO_2$).

The hydraulic flow rates calculated using the available standard setups on the circulator system (hereafter named level I, II, III), and their variations at increasing flow of injected CO_2 gas were measured. As shown in Table 1, the experimental results showed that, without any gas injection, the hydraulic flow varies greatly from 4 L min^{-1} for the lower configuration of the circulator to values of 14 and 18 L min^{-1} for level II and level III, respectively. The calculated liquid flow velocity (U_L) within the alveoli is 0.17, 0.60 and 0.77 m s^{-1} at level I, II and III, respectively.

Table 1: Variation of hydraulic flow rates according to the manually chosen level of the hydraulic circulator and the CO_2 flow injection. Liquid flow rates for the higher levels of the circulation system, at low CO_2 flow rates, were not measured assuming a negligible reduction of the rates according to the data for level I. Liquid flow rates (L min^{-1}) are shown as the average of three replicates ± standard deviation. U_L = liquid flow velocity (m s^{-1}).

	Liquid flow rate [L min^{-1}]		
CO_2 flow rate [NL min^{-1}]	**Circulator level I U_L = 0.17 m s^{-1}**	**Circulator level II U_L = 0.60 m s^{-1}**	**Circulator level III U_L = 0.77 m s^{-1}**
None	4.05 ± 0.03 (100%)	14.11 ± 0.15 (100%)	18.10 ± 0.33 (100%)
0.06	3.66 ± 0.11 (90.4%)	n.d.	n.d.
0.12	3.69 ± 0.09 (91.1%)	n.d.	n.d.
0.48	3.58 ± 0.02 (88.4%)	13.52 ± 0.31 (95.8%)	n.d.
0.60	3.62 ± 0.05 (89.4%)	11.23 ± 0.61 (79.6%)	n.d.
0.84	n.d.	8.61 ± 0.09 (61%)	18 ± 0.05 (99.4%)
1.08	n.d.	n.d.	16.95 ± 0.56 (93.6%)

Since the CO_2 is injected immediately upstream the circulator, the hydraulic flow is affected by the gas flow, and it is reduced as the gas flow rate increases. This is mostly evident at the level II of the circulator. Gas flow rates above 0.48 NL min^{-1} reduce the hydraulic flow rate to values below the 90% of the hydraulic load without CO_2 injection. On the contrary, the liquid flow rate at level III (18 L min^{-1}) is not significantly reduced by even higher CO_2 rates. Whereas no significant reductions in the liquid flow occur at the lower configuration of the circulator (level I). In the latter case, the low liquid flow (4 L min^{-1}) could favor a gas leak toward the tank rather than being swallowed up by the circulator and dissolved within the bulk flow to the hydraulic panels.

3.2 Mixing characterization

The mixing time (t_m) has been calculated at the three nominal liquid velocities, without CO_2 gas injection, to identify the relationship between t_m and U_L in the characterized cultivation system. The data showed that, by increasing the liquid velocity from 0.17 m s^{-1} (level I) to 0.60 m s^{-1} (level II), the mixing time decreases from 814 s to 246 s. Whereas above U_L = 0.60 m s^{-1} the slope of the curve decreases, and the t_m is not consistently reduced (194 s) (Fig. 3). The best fitting curve of the experimental data has an exponential trend (Fig. 3).

The computed energy consumption for the fluid handling at the three different liquid velocities was calculated to be 46, 27 and 38 Wh m^{-3}, respectively. Therefore, the reported power consumption values suggest that working at U_L values above 0.60 m s^{-1}, the inflexion point of t_m and U_L curve, is energetically disadvantageous since mixing time remains comparable with the one measured at 0.60 m s^{-1} (level II).

The reactor hydrodynamic behavior of other flat panel PBRs described in literature is based on different engineering solutions that affect hydrodynamic characteristics (Massart et al., 2014; Sierra et al., 2008). The authors reported the trend of mixing time in correlation with the gas velocity which drives the liquid handling. In the PBR prototype here described, the photosynthetic loop can be assimilated mainly to a plug flow reactor, although a continued stirred situation may be assumed since the estimated Reynolds number within the alveoli (*Re* ~ 10,000) indicates a turbulent state. Meanwhile, the mixing tank can be described as a CSTR (Continued Stirred Tank Reactor). Despite the different liquid handling solution, adopted in this study, with respect to the reported literature, the t_m values measured at 0.60 (level II) and 0.77 m s^{-1} (level III) fall into the ranges of mixing times reported in the above-mentioned works (Massart et al., 2014; Sierra et al., 2008).

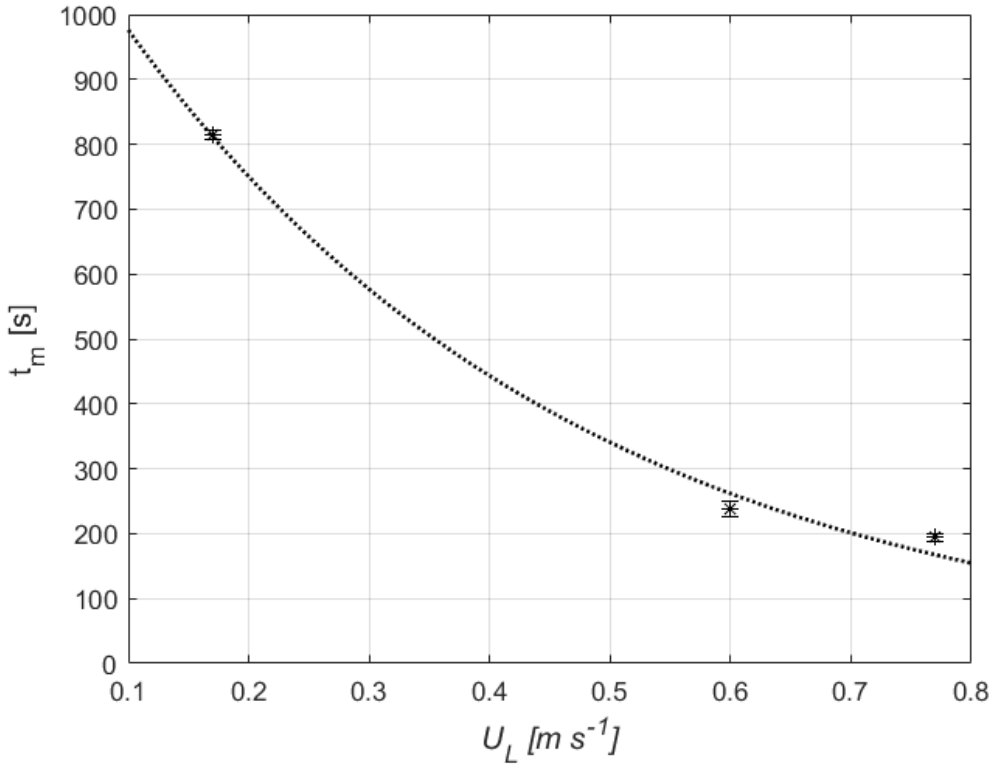

Figure 3: Influence of liquid flow velocity on mixing time. Data are shown as the average of three replicates ± standard deviation. Dotted line represents the exponential fitting (R^2 = 0.9946) obtained with the software Matlab®.

3.3 CO_2 mass transfer

Carbon dioxide uptake is one of the main target of microalgae cultivation technologies exploitation, therefore the CO_2 mass transfer coefficient ($k_La CO_2$) in the new PBR prototype was investigated. As described in section [2.1], CO_2 is directly injected upstream of the circulation system and the bubbles are swallowed up and broken by the circulator to smaller sizes. Moreover, the gas circulates within the fluid in the flat panels with a CO_2 bubbles residence time that is linked to the total length of the alveoli in the photostage loop (around 40 m).

The injection of CO_2 causes a reduction in the hydraulic flow rate since the gas flow interferes with the liquid handling of circulator, as discussed in section [3.1]. Therefore, k_La values were not measured for the CO_2 flow rates reducing the hydraulic flow below

363 the 90% of nominal value (Table 1) and the results are reported in Table 2. As expected,
364 the data showed a significant increase of $k_La CO_2$ values from $1.21 \cdot 10^{-5}$ to $2.99 \cdot 10^{-4}$ s^{-1}
365 along with the increase of the CO_2 flow injected for each hydraulic flow. The lowest k_La
366 values, meaning a more efficient CO_2 mass transfer, were achieved at the lowest CO_2
367 flows (0.06 and 0.12 NL min^{-1}) for all the circulator flow rates. However, at the circulator
368 level I (0.17 m s^{-1}) the measurements of $k_La CO_2$ may be affected by a gas leak toward the
369 mixing tank. Furthermore, such low liquid flow velocity determines the longest mixing
370 time of the PBR system (section [3.2]), which could affect the microalgae growth *e.g.*, by
371 favoring the sedimentation of biomass. The decrease of $k_La CO_2$ at level III, with respect
372 to level II, can be justified by the higher speed of the pump that favors the breaking and
373 mixing of CO_2 gaseous bubbles. However, circulator level III (0.77 m s^{-1}) did not show a
374 relevant improvement of hydraulic and mass transfer performances and it has a higher
375 energy consumption with respect to circulator level II (section [3.2]). Therefore, the
376 circulator and CO_2 flow setups showing the best performances in term of hydrodynamics,
377 CO_2 mass transfer and energy consumption were identified to be circulator level II with
378 the injection of CO_2 flow rates of 0.06 and 0.12 NL min^{-1}.
379 In the presented prototype, being the system's hydrodynamics based on a mechanical
380 circulation of the liquid, there is no need to inject air to support the movement of the
381 liquid culture and guarantee a certain degree of mixing and gas transfers. Thus, it is
382 possible to inject only pure low CO_2 flow rates achieving a high solubilization in the
383 photostage loop. In this way, CO_2 losses in atmosphere are limited, and the only cost to
384 obtain an efficient mixing and gas transfer is the one associated to the hydraulic circulator,
385 as in real scale application pure CO_2 comes already pressurized by previous industrial
386 stages. In literature, few examples of $k_La CO_2$ experimental measurements were reported.
387 The only comparisons with the system described in this work can be done against flat
388 panel air-lift PBRs (Chen et al., 2016; Massart et al., 2014). In these works, the authors

have used gas for the liquid-biomass mixing, and the reported $k_La CO_2$ values were higher (lower CO_2 solubilization) with respect to the data showed in the present manuscript.

Table 2: Dependency of CO_2 gas-liquid mass transfer coefficient (k_La) on the liquid flow velocities and CO_2 flow rates tested.

	k_La **CO₂ [s^{-1}]**		
CO_2 flow rate [NL min^{-1}]	**Circulator level I * U_L = 0.17 m s^{-1}**	**Circulator level II U_L = 0.60 m s^{-1}**	**Circulator level III U_L = 0.77 m s^{-1}**
0.06	$1.21 \cdot 10^{-5}$	$1.89 \cdot 10^{-5}$	$1.64 \cdot 10^{-5}$
0.12	$1.47 \cdot 10^{-5}$	$3.43 \cdot 10^{-5}$	$3.20 \cdot 10^{-5}$
0.48	n.d.	$1.30 \cdot 10^{-4}$	$1.24 \cdot 10^{-4}$
1.08	n.d.	n.d.	$2.99 \cdot 10^{-4}$

* k_La values for level I may be affected by the leak of CO_2 toward the tank (see section [3.1]).

The configuration of the presented PBR applies an innovative liquid handling solution that makes difficult to directly compare it with other flat panel PBRs described in literature, in terms of hydrodynamics and mass transfer efficiencies. Nevertheless, comparisons could be possible by addressing the problem from an energy point of view, in terms of energy required per unit volume operating in the unit of time.

In the PBR here described, the energy consumption related to the substrate handling was evaluated as effective power (at the wall socket) amounting to 27 Wh m^{-3} for level II of the hydraulic circulator, without any further cost associated to the CO_2 supply and stripping-out of O_2.

On the contrary, in the majority of flat panel PBRs described in literature, air is injected directly from the bottom of the flat-panels with the triple function of provide adequate mixing, CO_2 and favour the stripping-out of O_2. Therefore, the air supply parameter governs the energy consumption and the mass transfer capacity (Leupold et al., 2013; Sierra et al., 2008). A large volume of compressed air is therefore consumed to achieve the described triple function.

A power supply of 53 W m^{-3} was estimated by Sierra et al., (2008) to reach a mass transfer rate high enough to avoid excessive O_2 accumulation. More recently, Li et al., (2014) proposed a new design of flat panel PBR coupled to an external airlift module to overcome the major limitation of the mixing and improve the energy efficiency of the process by estimating a power supply of 31.6 W m^{-3}. However, the effective energy consumption of the system must include the efficiency of the associated air compressor, as also highlighted by Norsker et al., (2012). Therefore, direct comparisons with traditional flat-panel PBRs are difficult due to the absence of gross energy data concerning the power consumption of compressed air flat panels.

3.4 Light homogeneity

The lighting exposure (natural or artificial light) in photoautotrophic cultivation systems is a major factor influencing the performances of the process. Therefore, in the present study, we investigated the homogeneity of the artificial lighting system of the PBR prototype in order to assess the average light intensity at which microalgae cells are exposed. Light measurements on the surface exposed to the incident light have been used to build up a radiant matrix [Fig. 4]. The computation of the different measurements on the surface established a mean incident light intensity of 120 µmol m^{-2} s^{-1} with a light uniformity coefficient U_I of 40%. The trend of light distribution presents a wave shape, with the peaks corresponding to the fluorescent tubes positioning along the surface. Considering the light uniformity coefficient of 40%, a linear liquid velocity of 0.60 m s^{-1} (level II), and the length of each alveolus within the flat-panels (around 1.5 m), microalgae cells take about 10 s to move between two adjacent light intensity peaks. Therefore, it can be concluded that light fluctuations within the photostage loop do not significantly affect the overall biomass growth performance.

435 The use of fluorescent tubes as artificial lighting system has some disadvantages.
436 Fluorescent tubes are omnidirectional light sources, emitting at 360°. Therefore, only half
437 of the emitted light is directed to the microalgae suspension, whereas the other half might
438 need to be redirected to the desired area with the use of reflecting surfaces, requiring
439 additional accessory parts. Moreover, their emitting light intensity, as well as the light
440 spectrum quality, cannot be tuned if not by increasing the number of tubes (for the light
441 intensity).

442 The energy consumption of the lighting system, measured as described in section [2.8],
443 was found to be 455 Wh, a value which must be considered in order to estimate the global
444 efficiencies of the cultivation system, and to investigate alternative artificial light sources
445 to overcome the above-reported disadvantages reducing the energy requirements.

446 Further investigations are undergoing to evaluate the implementation of Light Emitting
447 Diodes (LEDs) as directional light source, due to their overall higher energy efficiency
448 compared to other commercially available lighting systems.

449

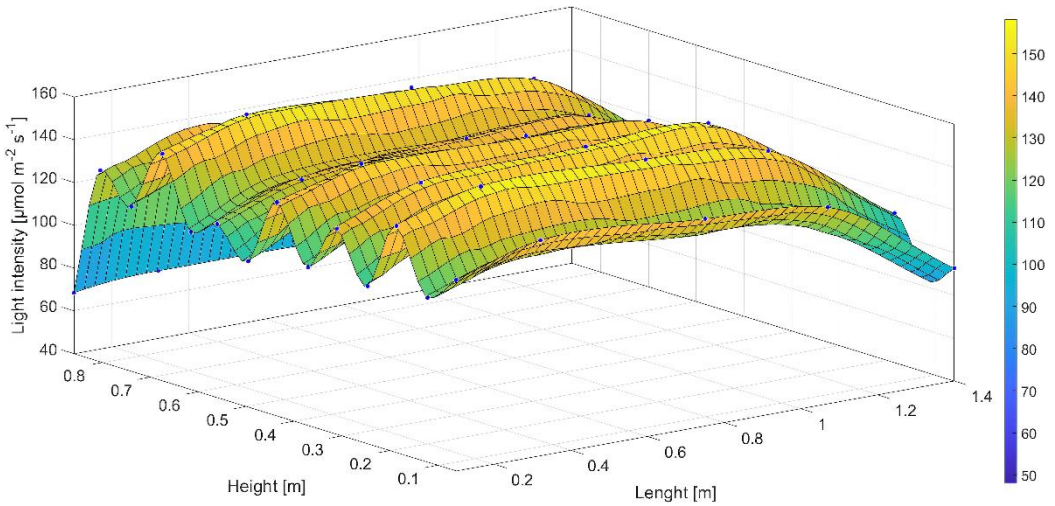

450

451 **Figure 4:** Graphical representation of the light intensity in a 3D space of the fluorescent
452 source. f(x,y) = piecewise cubic surface computed with the software Matlab® from p
453 (structure coefficient), where x is normalized by mean 0.728 and std 0.4788 and where y
454 is normalized by mean 0.4625 and std 0.2507.

3.5 Microalgae growth and CO_2 bio-fixation efficiency

Based on the data obtained for what concern the system's hydrodynamics and energy consumption, it has been decided to assess the growth of the green microalga *Acutodesmus obliquus* (*Scenedesmus obliquus*) operating at a liquid velocity of 0.60 m s^{-1} (level II) and with a CO_2 flow rate of 0.12 L min^{-1}. As mentioned in previous sections, these hydraulic parameters have been identified among the best performing setups. Moreover, it has been decided to work at constant dissolved CO_2 concentration of 25 mg L^{-1}, corresponding to a carbon dioxide partial pressure (P_{CO2}) of 0.017 bar. This value has been chosen to guarantee a relatively high CO_2/O_2 ratio, which may reduce the potential negative effects of O_2 accumulation via photorespiration, as suggested by (Sousa et al., 2012), and to assure a constant control on pH in the range between 7 and 7.5.

After 7 days of cultivation the cells reached a final concentration of 1.9 g L^{-1} (Fig. 5). The analysis of the growth curves showed a mean daily volumetric productivity (P_x) of 0.21 g L^{-1} d^{-1} ± 0.01 (n = 3). The CO_2 fixation yield (ηCO_2), calculated as in Eq. 5 and based on elemental composition analysis of *A. obliquus* previously performed in our laboratory with the same cultivation setup (C 53.8 %, H 8.88 %, O 37.3% by weight), accounted for the 64% of the total CO_2 injected.

The cultivation of *A. obliquus* was successful in the PBR, and an axenic homogeneous cell culture could be developed to high cell concentrations. Using fluorescent microscopy, microalgae cells were found in good shape for the whole batch cultivation (data not shown), indicating no apparent shear stress despite the use of the mechanical circulating device set to obtain U_L = 0.60 m s^{-1}. Finally, as shown in section [3.2], the average light intensity on the surface of the flat panels was about 120 µmol m^{-2} s^{-1}, and the biomass yield on light energy ranged from 0.3 to 0.6 g mol^{-1} during the whole cultivation period,

480 values comparable with data reported for several green microalgae grown in flat panel
481 reactors (Kliphuis et al., 2010; Li et al., 2014).
482 A recently published review by Lim and co-authors extensively analyzed the CO_2 bio-
483 fixation results available in literature (Lim et al., 2021). The authors analyzed several
484 approaches to evaluate the effective CO_2 bio-fixation by microalgae culture and reported
485 that most of the scientific literature investigated the CO_2 fixation only at laboratory scale.
486 In this work, for CO_2 bio-fixation calculations we used the elementary analysis approach.
487 Moreover, the experiments described in this work were performed on volumes higher
488 than laboratory scale, and additionally a pure CO_2 stream was used to feed the PBR in a
489 way that could be compatible with already available industrial streams. The obtained
490 results place the new flat-panel PBR among the most promising prototypal technology to
491 implement a microalgae CO_2 fixation approach at industrial scale. Furthermore, the
492 hardware components of the PBR, equipped with a multi-probes system connected via
493 transductor to an integrated PLC (see section [2.1]), make this pilot-scale prototype
494 already suitable for remote monitoring and control of cultivation parameters to
495 incorporate the Internet of Things (IoT). This, as extensively highlighted in recent
496 literature, is becoming a relevant aspect as both academic research and industry are
497 gradually moving towards process automation and remote operation (Tham et al., 2022;
498 Wang et al., 2022).

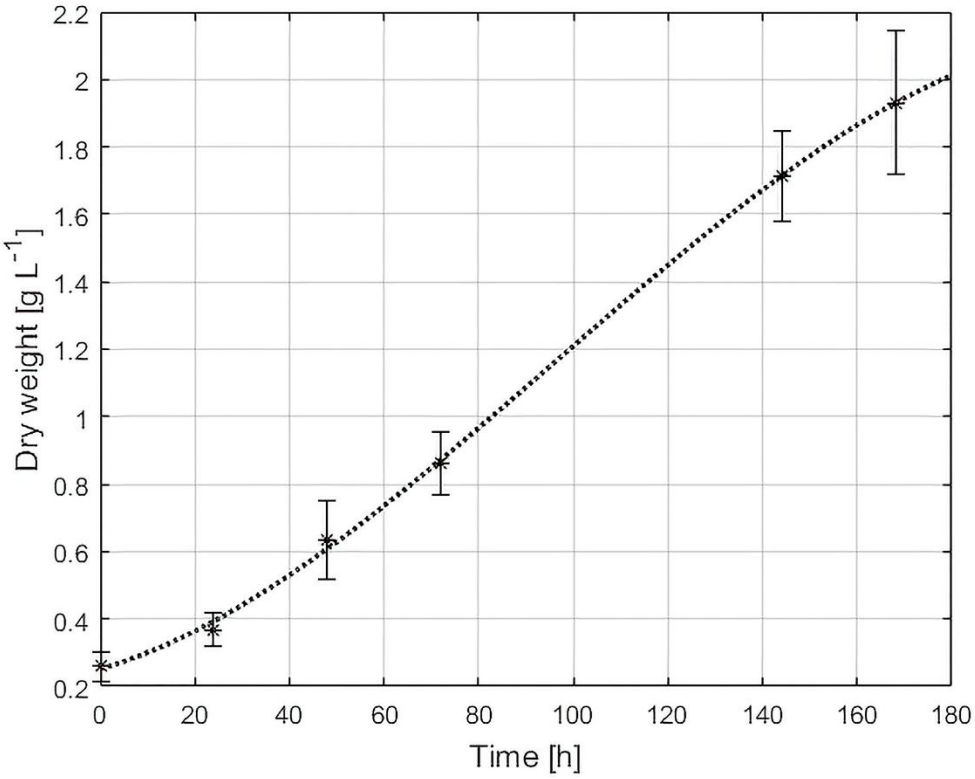

Figure 5: Biomass concentration of *Acutodesmus obliquus* in the flat panel photobioreactor. Stars represent the dry weight measurements ± standard deviation (n = 3). Dotted line represents the third-degree polynomial interpolation (R^2 = 0.9985) obtained with the software Matlab®.

4. Conclusion

This study provides the characterization of a new flat panel PBR prototype regarding the main hydrodynamic parameters, the CO_2 supply strategy and the artificial lighting system. An innovative liquid handling strategy based on a pump-assisted circulation has been proposed and tested in this work. The liquid culture is moved by a centrifugal pump that allows to achieve appropriate culture mixing and enhance CO_2 mass transfer with a lower power consumption compared to the majority of flat-panels described in the literature. The biological performances of the system have been successfully tested by cultivating the green microalga *Acutodesmus obliquus*, which showed a mean daily volumetric productivity (P_x) of 0.21 g L^{-1} d^{-1} and a biomass yield on light energy comparable to those reported for several green microalgae in flat-panel PBRs.

Furthermore, the CO_2 bio-fixation efficiency was found to be higher (64%) than those reported in literature for several microalgae species grown in large-scale setups. Taken all together, the energetic and biological performances of this pilot-scale PBR may constitute an important step toward the development of industrial-scale technologies to mitigate CO_2 while obtaining high quality microalgal biomass. Future work will be carried out in order to further reduce the energy consumption, optimize CO_2 and light supply strategies, as well as several other cultivation parameters (e.g., media composition, temperature, light quality), to further optimize the overall photobioreactor CapEx and OpEx.

Declaration of Competing Interest

The authors declare that the research was conducted in the absence of any commercial or financial relationships that could be construed as a potential conflict of interest.

Acknowledgements

This work was supported by Politecnico di Torino and the Wearwe group @PoliTo (58_DIM21RIGVIN; 58_RCE19ZANMAR_03). The authors are grateful to Arcobaleno Cooperativa Sociale (Torino, Italy) in the person of F. Passarelli and F. De Bernardi for their technical support.

Author contributions

M.C., A.O., M.Z. and V.A.R. designed research; M.C., D.A., V.C., and C.D. performed research; M.C .and V.C. analysed data; M.C. and V.A.R. wrote the article.

References

Acién, F.G., Fernández, J.M., Magán, J.J., Molina, E., 2012. Production cost of a real microalgae production plant and strategies to reduce it. Biotechnology Advances 30, 1344–1353. https://doi.org/10.1016/j.biotechadv.2012.02.005

Acién, F.G., Molina, E., Reis, A., Torzillo, G., Zittelli, G.C., Sepúlveda, C., Masojídek, J., 2017. Photobioreactors for the production of microalgae, Microalgae-Based Biofuels and Bioproducts: From Feedstock Cultivation to End-Products. https://doi.org/10.1016/B978-0-08-101023-5.00001-7

Adesanya, V.O., Cadena, E., Scott, S.A., Smith, A.G., 2014. Life cycle assessment on microalgal biodiesel production using a hybrid cultivation system. Bioresource Technology 163, 343–355. https://doi.org/10.1016/j.biortech.2014.04.051

Benemann, J., 2013. Microalgae for biofuels and animal feeds. Energies (Basel) 6, 5869–5886. https://doi.org/10.3390/en6115869

Blunden, J., Boyer, T., 2021. State of the climate in 2020. Bull Am Meteorol Soc. https://doi.org/10.1175/2021BAMSStateoftheClimate.1

Brown, L.M., Zeiler, K.G., 1993. Aquatic biomass and carbon dioxide trapping. Energy Conversion and Management 34, 1005–1013. https://doi.org/10.1016/0196-8904(93)90048-F

Carlsson, A.S., van Beilen, J.B., Möller, R., Clayton, D., 2007. Micro- and Macro-algae: Utility for Industrial Applications. Outputs from the EPOBIO Project. CPL Press, Berks.

Carvalho, A.P., Meireles, L.A., Malcata, F.X., 2006. Microalgal Reactors: A Review of Enclosed System Designs and Performances. Biotechnol Prog 22, 1490–1506. https://doi.org/10.1021/bp060065r

Cheah, W.Y., Show, P.L., Chang, J.S., Ling, T.C., Juan, J.C., 2015. Biosequestration of atmospheric CO2 and flue gas-containing CO2 by microalgae. Bioresource Technology 184, 190–201. https://doi.org/10.1016/j.biortech.2014.11.026

Chen, Z., Jiang, Z., Zhang, X., Zhang, J., 2016. Numerical and experimental study on the CO2 gas-liquid mass transfer in flat-plate airlift photobioreactor with different baffles. Biochemical Engineering Journal 106, 129–138. https://doi.org/10.1016/j.bej.2015.11.011

Chiaramonti, D., Prussi, M., Casini, D., Tredici, M.R., Rodolfi, L., Bassi, N., Zittelli, G.C., Bondioli, P., 2013. Review of energy balance in raceway ponds for microalgae cultivation: Re-thinking a traditional system is possible. Applied Energy 102, 101–111. https://doi.org/10.1016/j.apenergy.2012.07.040

Chini Zittelli, G., Rodolfi, L., Bassi, N., Biondi, N., Tredici, M.R., 2013. Photobioreactors for microalgae biofuel production, in: Borowitzka, M.A., Moheimani, N.R. (Eds.), Algae for Biofuels and Energy. Springer, Dodrecht., pp. 115–131. https://doi.org/10.1007/978-94-007-5479-9

Chisti, Y.M., 1989. Airlift Bioreactors. Elsevier, London.

Cuaresma, M., Janssen, M., Vílchez, C., Wijffels, R.H., 2009. Productivity of Chlorella sorokiniana in a short light-path (SLP) panel photobioreactor under high irradiance. Biotechnology and Bioengineering 104, 352–359. https://doi.org/10.1002/bit.22394

De Vree, J.H., Bosma, R., Janssen, M., Barbosa, M.J., Wijffels, R.H., 2015. Comparison of four outdoor pilot-scale photobioreactors. Biotechnology for Biofuels 8, 1–12. https://doi.org/10.1186/s13068-015-0400-2

del Rio-Chanona, E.A., Wagner, J.L., Ali, H., Fiorelli, F., Zhang, D., Hellgardt, K., 2019. Deep learning-based surrogate modeling and optimization for microalgal biofuel production and photobioreactor design. AIChE Journal 65, 915–923. https://doi.org/10.1002/aic.16473

595 Estrada-Graf, A., Hernández, S., Morales, M., 2020. Biomitigation of CO2 from flue
596 gas by Scenedesmus obtusiusculus AT-UAM using a hybrid photobioreactor
597 coupled to a biomass recovery stage by electro-coagulation-flotation.
598 Environmental Science and Pollution Research.
599 https://doi.org/10.1007/s11356-020-08240-2
600 Francisco, É.C., Neves, D.B., Jacob-Lopes, E., Franco, T.T., 2010. Microalgae as
601 feedstock for biodiesel production: Carbon dioxide sequestration, lipid
602 production and biofuel quality. Journal of Chemical Technology and
603 Biotechnology 85, 395–403. https://doi.org/10.1002/jctb.2338
604 Gimpel, J.A., Henríquez, V., Mayfield, S.P., 2015. In metabolic engineering of
605 eukaryotic microalgae: Potential and challenges come with great diversity.
606 Frontiers in Microbiology 6, 1–14.
607 https://doi.org/10.3389/fmicb.2015.01376
608 Goli, A., Shamiri, A., Talaiekhozani, A., Eshtiaghi, N., Aghamohammadi, N., Aroua,
609 M.K., 2016. An overview of biological processes and their potential for CO2
610 capture. Journal of Environmental Management.
611 https://doi.org/10.1016/j.jenvman.2016.08.054
612 Greenwell, H.C., Laurens, L.M.L., Shields, R.J., Lovitt, R.W., Flynn, K.J., 2010. Placing
613 microalgae on the biofuels priority list: A review of the technological
614 challenges. Journal of the Royal Society Interface 7, 703–726.
615 https://doi.org/10.1098/rsif.2009.0322
616 Jorquera, O., Kiperstok, A., Sales, E.A., Embiruçu, M., Ghirardi, M.L., 2010.
617 Comparative energy life-cycle analyses of microalgal biomass production in
618 open ponds and photobioreactors. Bioresource Technology 101, 1406–
619 1413. https://doi.org/10.1016/j.biortech.2009.09.038
620 Khan, S.A., Rashmi, Hussain, M.Z., Prasad, S., Banerjee, U.C., 2009. Prospects of
621 biodiesel production from microalgae in India. Renewable and Sustainable

622 Energy Reviews 13, 2361–2372.
623 https://doi.org/10.1016/j.rser.2009.04.005
624 Kliphuis, A.M.J., de Winter, L., Vejrazka, C., Martens, D.E., Janssen, M., Wijffels, R.H.,
625 2010. Photosynthetic efficiency of Chlorella sorokiniana in a turbulently
626 mixed short light-path photobioreactor. Biotechnology Progress 26, 687–
627 696. https://doi.org/10.1002/btpr.379
628 Leupold, M., Hindersin, S., Kerner, M., Hanelt, D., 2013. The effect of discontinuous
629 airlift mixing in outdoor flat panel photobioreactors on growth of
630 Scenedesmus obliquus. Bioprocess and Biosystems Engineering 36, 1653–
631 1663. https://doi.org/10.1007/s00449-013-0939-x
632 Li, J., Stamato, M., Velliou, E., Jeffryes, C., Agathos, S.N., 2014. Design and
633 characterization of a scalable airlift flat panel photobioreactor for
634 microalgae cultivation. Journal of Applied Phycology 27, 75–86.
635 https://doi.org/10.1007/s10811-014-0335-1
636 Lim, Y.A., Chong, M.N., Foo, S.C., Ilankoon, I.M.S.K., 2021. Analysis of direct and
637 indirect quantification methods of CO2 fixation via microalgae cultivation in
638 photobioreactors: A critical review. Renewable and Sustainable Energy
639 Reviews 137, 110579. https://doi.org/10.1016/j.rser.2020.110579
640 López-Rosales, L., Sánchez-Mirón, A., Contreras-Gómez, A., García-Camacho, F.,
641 Battaglia, F., Zhao, L., Molina-Grima, E., 2019. Characterization of bubble
642 column photobioreactors for shear-sensitive microalgae culture.
643 Bioresource Technology 275, 1–9.
644 https://doi.org/10.1016/j.biortech.2018.12.009
645 Massart, A., Mirisola, A., Lupant, D., Thomas, D., Hantson, A.L., 2014. Experimental
646 characterization and numerical simulation of the hydrodynamics in an airlift
647 photobioreactor for microalgae cultures. Algal Research 6, 210–217.
648 https://doi.org/10.1016/j.algal.2014.07.003

649 Norsker, H., Barbosa, M.J., Vermuë, M.H., Wijffels, R.H., 2012. On Energy Balance
650 and Production Costs in Tubular and Flat Panel Photobioreactors. TATuP -
651 Zeitschrift für Technikfolgenabschätzung in Theorie und Praxis 21, 54–62.
652 https://doi.org/10.14512/tatup.21.1.54
653 Norsker, N.H., Barbosa, M.J., Vermuë, M.H., Wijffels, R.H., 2011. Microalgal
654 production - A close look at the economics. Biotechnology Advances 29, 24–
655 27. https://doi.org/10.1016/j.biotechadv.2010.08.005
656 Pandey, A., Lee, D.J., Chisti, Y., Soccol, C.R., 2014. Biofuels From Algae Biofuels
657 From. Elsevier, Amsterdam.
658 Perin, G., Simionato, D., Bellan, A., Carone, M., Occhipinti, A., Maffei, M.E.,
659 Morosinotto, T., 2017. Cultivation in industrially relevant conditions has a
660 strong influence on biological properties and performances of
661 Nannochloropsis gaditana genetically modified strains. Algal Research 28,
662 88–99. https://doi.org/10.1016/j.algal.2017.10.013
663 Reyna-Velarde, R., Cristiani-Urbina, E., Hernández-Melchor, D.J., Thalasso, F.,
664 Cañizares-Villanueva, R.O., 2010. Hydrodynamic and mass transfer
665 characterization of a flat-panel airlift photobioreactor with high light path.
666 Chemical Engineering and Processing: Process Intensification 49, 97–103.
667 https://doi.org/10.1016/j.cep.2009.11.014
668 Rodolfi, L., Zittelli, G.C., Bassi, N., Padovani, G., Biondi, N., Bonini, G., Tredici, M.R.,
669 2009. Microalgae for oil: Strain selection, induction of lipid synthesis and
670 outdoor mass cultivation in a low-cost photobioreactor. Biotechnology and
671 Bioengineering 102, 100–112. https://doi.org/10.1002/bit.22033
672 Rosenberg, J.N., Mathias, A., Korth, K., Betenbaugh, M.J., Oyler, G.A., 2011.
673 Microalgal biomass production and carbon dioxide sequestration from an
674 integrated ethanol biorefinery in Iowa: A technical appraisal and economic
675 feasibility evaluation. Biomass and Bioenergy 35, 3865–3876.
676 https://doi.org/10.1016/j.biombioe.2011.05.014

677 Sierra, E., Acién, F.G., Fernández, J.M., García, J.L., González, C., Molina, E., 2008.
678 Characterization of a flat plate photobioreactor for the production of
679 microalgae. Chemical Engineering Journal 138, 136–147.
680 https://doi.org/10.1016/j.cej.2007.06.004
681 Slade, R., Bauen, A., 2013. Micro-algae cultivation for biofuels: Cost, energy
682 balance, environmental impacts and future prospects. Biomass and
683 Bioenergy 53, 29–38. https://doi.org/10.1016/j.biombioe.2012.12.019
684 Solimeno, A., Gabriel, F., García, J., 2017. Mechanistic model for design, analysis,
685 operation and control of microalgae cultures: Calibration and application to
686 tubular photobioreactors. Algal Research 21, 236–246.
687 https://doi.org/10.1016/j.algal.2016.11.023
688 Sousa, C., de Winter, L., Janssen, M., Vermuë, M.H., Wijffels, R.H., 2012. Growth of
689 the microalgae Neochloris oleoabundans at high partial oxygen pressures
690 and sub-saturating light intensity. Bioresource Technology 104, 565–570.
691 https://doi.org/10.1016/j.biortech.2011.10.048
692 Stanier, R.Y., Kunisawa, R., Mandel, M., Cohen-Bazire, G., 1971. Purification and
693 properties of unicellular blue-green algae (order Chroococcales). Bacteriol
694 Rev 35, 171–205. https://doi.org/10.1128/mmbr.35.2.171-205.1971
695 Tan, C.H., Tan, X., Ho, S.H., Lam, S.S., Show, P.L., Nguyen, T.H.P., 2020. Conceptual
696 design of a hybrid thin layer cascade photobioreactor for microalgal
697 biodiesel synthesis. International Journal of Energy Research 44, 9757–
698 9771. https://doi.org/10.1002/er.5699
699 Tham, P.E., Ng, Y.J., Vadivelu, N., Lim, H.R., Khoo, K.S., Chew, K.W., Show, P.L., 2022.
700 Sustainable smart photobioreactor for continuous cultivation of microalgae
701 embedded with Internet of Things. Bioresource Technology 346.
702 https://doi.org/10.1016/j.biortech.2021.126558

703 Torzillo, G., Pushparaj, B., Masojidek, J., Vonshak, A., 2003. Biological constraints
704 in algal biotechnology. Biotechnology and Bioprocess Engineering 8, 338–
705 348. https://doi.org/10.1007/BF02949277
706 Torzillo, G., Zittelli, G.C., 2015. Tubular Photobioreactors, in: Prokop, A., Bajpai,
707 R.K., Zappi, M.E. (Eds.), Algal Biorefineries. In: Products and Refinery Design,
708 Vol. 2. Springer, Switzerland, pp. 187–212. https://doi.org/10.1007/978-3-
709 319-20200-6
710 Tredici, M.R., Bassi, N., Prussi, M., Biondi, N., Rodolfi, L., Chini Zittelli, G.,
711 Sampietro, G., 2015. Energy balance of algal biomass production in a 1-ha
712 "Green Wall Panel" plant: How to produce algal biomass in a closed reactor
713 achieving a high Net Energy Ratio. Applied Energy 154, 1103–1111.
714 https://doi.org/10.1016/j.apenergy.2015.01.086
715 Tredici, M.R., Chini Zittelli, G., Rodolfi, L., 2010. Photobioreactors, in: Flickinger,
716 M.C. (Ed.), Encyclopedia of Industrial Biotechnology: Bioprocess,
717 Bioseparation, and Cell Technol- Ogy. Wiley, Hoboken, NJ, pp. 3821–3838.
718 https://doi.org/10.1002/9780470054581.eib479
719 Vanthoor-Koopmans, M., Wijffels, R.H., Barbosa, M.J., Eppink, M.H.M., 2013.
720 Biorefinery of microalgae for food and fuel. Bioresource Technology 135,
721 142–149. https://doi.org/10.1016/j.biortech.2012.10.135
722 Vasile, N.S., Cordara, A., Usai, G., Re, A., 2021. Computational analysis of dynamic
723 light exposure of unicellular algal cells in a flat-panel photobioreactor to
724 support light-induced CO2 bioprocess development. Frontiers in
725 Microbiology 12. https://doi.org/10.3389/fmicb.2021.639482
726 Wang, K., Khoo, K.S., Leong, H.Y., Nagarajan, D., Chew, K.W., Ting, H.Y., Selvarajoo,
727 A., Chang, J.S., Show, P.L., 2022. How does the Internet of Things (IoT) help
728 in microalgae biorefinery? Biotechnology Advances.
729 https://doi.org/10.1016/j.biotechadv.2021.107819

730 Weise, T., Reinecke, J.M., Schuster, S., Pfaff, M., 2019. Optimizing turbidostatic
731 microalgal biomass productivity: A combined experimental and coarse-
732 grained modelling approach. Algal Research 39.
733 https://doi.org/10.1016/j.algal.2019.101439
734 Yadav, G., Karemore, A., Dash, S.K., Sen, R., 2015. Performance evaluation of a
735 green process for microalgal CO2 sequestration in closed photobioreactor
736 using flue gas generated in-situ. Bioresource Technology 191, 399–406.
737 https://doi.org/10.1016/j.biortech.2015.04.040
738 Yadav, G., Sen, R., 2017. Microalgal green refinery concept for biosequestration of
739 carbon-dioxide vis-à-vis wastewater remediation and bioenergy
740 production: Recent technological advances in climate research. Journal of
741 CO2 Utilization 17, 188–206. https://doi.org/10.1016/j.jcou.2016.12.006
742 Yang, C., Mao, Z.-S., 2014. Airlift loop reactors, in: Yang, C., Zai-Sha, M. (Eds.),
743 Numerical Simulation of Multiphase Reactors with Continuous Liquid Phase.
744 pp. 153–229. https://doi.org/10.1016/b978-0-08-099919-7.00004-4
745